ChemComm

Accepted Manuscript

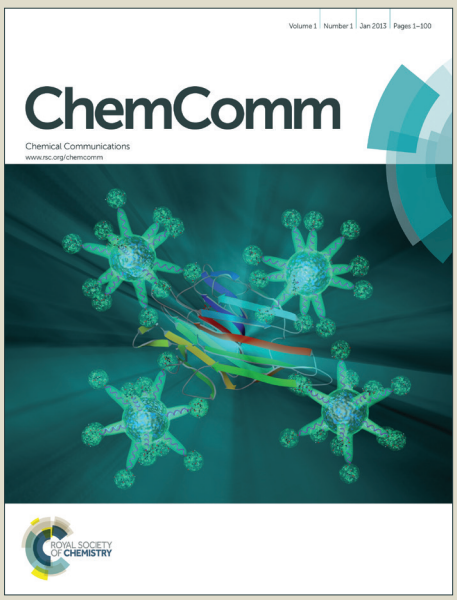

ROYAL SOCIETY OF CHEMISTRY

www.rsc.org/chemcomm

ChemComm

RSCPublishing

COMMUNICATION

H_2 Spillover Enhanced Hydrogenation Capability of TiO_2 Used for Photocatalytic Splitting of Water: A Traditional Phenomenon for New Application

Cite this: DOI: 10.1039/x0xx00000x

Received 00th January 2012,
Accepted 00th January 2012

DOI: 10.1039/x0xx00000x

www.rsc.org/

Yingming Zhu, Dongsheng Liu, Ming Meng *

Black TiO_2 was usually obtained *via* hydrogenation at high pressure and high temperature. Herein, we reported a facile hydrogenation of TiO_2 in the presence of a small amount of Pt at relatively low temperature and atmospheric pressure. The hydrogen spillover from Pt to TiO_2 accounts well for the greatly enhanced hydrogenation capability. The as-synthesized Pt/TiO_2 exhibits remarkably improved photocatalytic activity for water splitting.

As an excellent photocatalyst for hydrogen generation and water treating[1] , titanium dioxide (TiO_2) has drawn extensive attention. However, the wide-band-gap of TiO_2 makes it only respond to ultraviolet light. To improve the solar energy utilization efficiency, many strategies on band structure modification such as doping nonmetal[2] or metal[3] elements have been proposed to reduce the band gap of TiO_2. Recently, black TiO_2 has attracted enormous attention for its high absorptivity to visible/infrared light and high photocatalytic activity [4]. By now, the synthesis of "disorder-engineered'' black TiO_2 has become a research hotspot[5]. Nevertheless, the reported hydrogenation methods have many disadvantages such as the requirements of high pressure and high temperature, and the ineffectiveness to crystalline TiO_2[5c] (e.g. Degussa P25). Meanwhile, it is shown that the hydrogenation on amorphous titania precursors cannot ensure good photocatalytic activity[6]. Hence, new strategies on TiO_2 hydrogenation should be developed.

Hydrogen spillover from noble metal nanoparticles (Pt, Pd, Ru or Rh) to supports is an often-observed phenomenon in many traditional catalytic reactions[7]. Generally, the H_2 molecules are first chemically adsorbed and dissociated into atomic species by metallic nanoparticles; then they migrate to supports, providing active species for catalytic reactions. If the supports are reducible oxides, hydrogen spillover can greatly enhance their reducibility. So, it is reasonable to imagine that the combination of noble metals and TiO_2 would improve the reducibility of TiO_2. However, the reported hydrogenation of TiO_2 to TiO_2@TiO_{2-x} was always performed in the absence of noble metals (e.g., Pt), which were later loaded on the after-hydrogenated TiO_2@TiO_{2-x} [4,5d]. As the function of hydrogen spillover is ignored, the reaction condition is often rigorous. To demonstrate the effectiveness of hydrogen spillover and make the reaction condition milder, we designed a facile hydrogenation route on crystalline TiO_2, in which Pt was preloaded on TiO_2; then hydrogenation was carried out on the precursor at atmospheric pressure and relatively low-temperature. The whole process is described in the route 2 of **Scheme 1**. For comparison, another sample Pt/TiO_2(H_2) was also prepared in a way similar to the widely reported route[4,5d] (route 1 of **Scheme 1**), using the hydrogenated TiO_2@TiO_{2-x} as support for the subsequent Pt loading. Herein, we surprisingly found that the as-designed hydrogenation route at the condition of atmospheric pressure and relatively low-temperature is feasible and highly efficient for the synthesis of Pt promoted TiO_2/TiO_{2-x} catalysts. Compared with the sample prepared *via* route 1, the catalyst obtained through route 2 is much more active for water splitting to produce H_2.

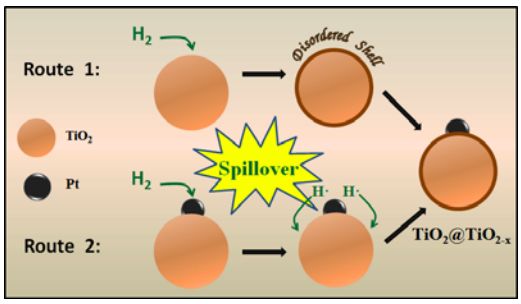

Scheme 1. Strategies for the hydrogenation of Pt promoted TiO_2 to obtain the TiO_2@TiO_{2-x}. Route 1: hydrogenation of TiO_2 followed by the loading of Pt; Route 2: hydrogen spillover involved simultaneous hydrogenation of Pt/TiO_2.

The precursor of the supported catalyst 1wt% Pt/P25 was first prepared *via* conventional impregnation, then it was reduced by sodium borohydride to get metallic Pt. The Pt nanoparticles possessing an average diameter < 3 nm are highly dispersed on P25 as seen in **Fig.1a.** H_2 temperature-programmed reduction (TPR) is a well-developed technology for the characterization on the reducibility of oxygen species[8]. So, the H_2-TPR was employed to evaluate the reducibility of

P25 & Pt/P25 before hydrogenation in order to select proper hydrogenation temperature, the results of which are shown in **Fig. 1b**. As expected, P25 can hardly react with H_2, showing very weak signal and no reduction peaks; while after preloading of metallic Pt, the reduction signal is greatly enhanced from 160 °C, forming four obvious peaks at 400, 500, 700 and 750 °C. On the basis of the H_2-TPR results, Pt/P25 was annealed in 8% H_2/N_2 atmosphere at several different temperatures (200, 400, 500 or 700 °C) for 4 h, respectively. The hydrogenated samples are denoted as Pt/P25-x; x stands for the treatment temperature.

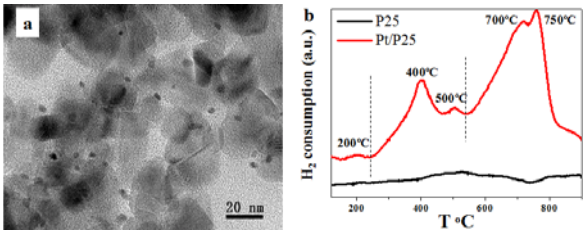

Figure 1. (a) TEM image of Pt/P25; (b) H_2-TPR profiles of P25 and Pt/P25.

To further determine the crystal structure and possible phase changes of these catalysts after hydrogenation, the XRD patterns were recorded. As illustrated in **Fig. S1a**, the catalysts treated at 200, 400 and 500 °C exhibit typical peaks of P25. For Pt/P25-700, the peaks of rutile nearly disappear, meaning the structural transformation of P25. What's more, for Pt/P25-500 and Pt/P25-700, a new peak at 30.4 ° is detected, which corresponds to Ti_3O_5 phase (JCPDS No. 27-0905). And for Pt/P25-700, another peak at 44.2 ° is observed as well, which is probably contributed by Ti_3Pt alloy phase (JCPDS No. 07-0353). Both the results of H_2-TPR and XRD suggest that above 240 °C the oxygen vacancy may be present in the catalysts due to the oxygen extraction by H_2. To further confirm the generation of oxygen vacancy, the electron paramagnetic resonance (EPR) spectra of the catalysts were recorded, as shown in **Fig S1b**. It can be seen that the catalysts Pt/P25-400 and Pt/P25-500 do show a strong EPR signal at g = 2.003, which is attributed to oxygen vacancy combined with one electron (denoted as $Vo^{\bullet}$)[9]; the EPR signal of Pt/P25-400 is a little stronger than that of Pt/P25-500, indicating the higher concentration of $Vo^{\bullet}$ in Pt/P25-400.

We also recorded the UV–vis diffuse reflectance spectra (UV-vis DRS) of the catalysts (**Fig. S2**). Compared with P25, the visible light absorption of Pt/P25 is enhanced due to the SPR effect of Pt nanoparticles. But the further improvement of visible light absorption is contributed to hydrogenation. The Pt/P25-400 presents both strong visible light absorption and band gap absorption. However, the UV-vis DRS of Pt/P25-700 is dramatically changed. The absence of band gap absorption verifies the destruction of P25 structure. For Pt/P25-500, though it has a band gap absorption, its visible light absorption is more similar to that of Pt/P25-700, as reflected by the small peak at ~500 nm marked by dash line box. This detail implies the initial breaking of the structure of P25 at 500 °C.

According to the results of H_2-TPR, XRD EPR and UV-vis DRS, the reaction of hydrogen with Pt/TiO_2 catalyst in different temperature range could be visualized as follows:

$$H_2 \xrightarrow[\text{Spillover}]{\text{Pt}} 2H\cdot \quad (1);$$

$$2H\cdot + 1/2O_{2\,(ads)} \longrightarrow H_2O \quad (2);$$

$$H\cdot + \sim \text{Ti-O-Ti-O} \sim \longrightarrow \sim\text{Ti-OH} + Vo^{\bullet}\text{-Ti-O}\sim \quad (3);$$

$$2H\cdot + 3TiO_2 \longrightarrow Ti_3O_5 + H_2O \quad (4);$$

(~ Ti or O ~ : any chemical bond linking to Ti or O; ~ Ti-O-Ti-O ~: surface lattice oxygen species)

(1) H_2 is firstly dissociated into H atoms by Pt (Eq. 1), then the adsorbed O_2 on the surface of TiO_2 is reduced to H_2O (Eq. 2) below 240 °C.

(2) Above 240 °C, the bond between surface lattice oxygen and Ti is interrupted by H atom, forming a hydroxyl group and an oxygen vacancy (Eq. 3)[10].

(3) As the temperature is further increased to 540 °C or higher, atomic H species would diffuse from surface into bulk, generating localized Ti–O(H)–Ti species[5d, 11]; after dehydration, a reduced form (Ti_3O_5) of titanium dioxide (Eq. 4) is produced.

Apparently, the H_2 spillover is involved in hydrogenation, which promotes the formation of TiO_2/TiO_{2-x}.

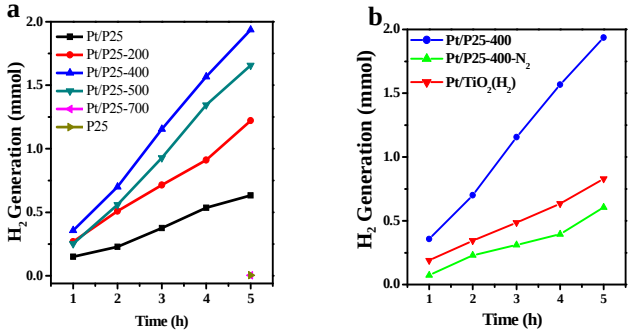

Figure 2. (a) Time-dependent H_2 production over Degussa P25, Pt/P25 and Pt/P25-x (x=200, 400, 500 or 700 °C) under simulated solar light; (b) time-dependent H_2 production over Pt/P25-400, Pt/P25-400(N_2) and Pt/P25(H_2) under simulated solar light.

The photocatalytic activity and stability of these catalysts for H_2 generation were investigated, as shown in **Fig. 2**. Compared with bare P25 and the Pt/P25 without hydrogenation, the H_2 generation ability of Pt/P25 hydrogenated at 200, 400 or 500 °C is greatly improved (**Fig. 2a**). The Pt/P25-400 possesses the best activity, showing a production of 1.936 mmol H_2 after 5 h irradiation, which is 3 times and 38 times to that of Pt/P25 and bare P25, respectively. To certify the function of H_2 spillover more clearly, two referential catalysts were prepared, namely, Pt/P25-400-N_2 and Pt/P25(H_2) (**Fig 2b**). The H_2 production rates of these two catalysts are in the same level as Pt/P25, but much lower than that for Pt/P25-400, which insinuates that the spillover is really a crucial factor to the high catalytic activity of Pt/P25-x. Meanwhile, the Pt/P25-400 also displays excellent stability during the cyclic durability tests, as shown in **Fig S3**.

To better understand the hydrogen spillover effect on the TiO_2 hydrogenation, the best catalyst Pt/P25-400 was selected for further investigation. The X-ray photoelectron spectroscopy (XPS) was used to characterize the change of surface chemical states of Pt/P25-400 by using P25 and Pt/P25 as references for comparison (**Fig. S4**). It is found that the XPS spectra of Ti*2p* (**Fig S4a**) and O*1s* (**Fig. S4b**) for P25 and Pt/P25 are almost identical, suggesting little effect of Pt loading on the chemical states of surface TiO_2. However, for Pt/P25-400, the Ti *2p* peaks appear at lower binding energy positions. By using a peak-fitting deconvolution, the O*1s* peak is deconvoluted into two peaks for all the detected samples. It is seen that before hydrogenation the surface lattice oxygen in Ti-O-Ti (529.5 eV) is the major O species on TiO_2 surface with a small amount of Ti-OH (surface hydroxyl, 532.0 eV) species present; after hydrogenation the O*1s* peak of Pt/P25-400 obviously shifts to lower binding energy position with the peak for Ti-OH species remarkably enhanced, which implies the increase of its surface concentration. These changes are in good agreement with the

former H_2-TPR analysis and the description in Eq. 3. The decrease of the binding energy for both Ti *2p* and O *1s* also suggests that the increase of surface electron density after hydrogenation.[12] This deduction is supported by the EPR results in which electron-rich species namely oxygen vacancy combined with one electron ($Vo^{\bullet}$) have been clearly detected.

The photoluminescence (PL) emission spectra of P25, Pt/P25 and Pt/P25-400 were also recorded (**Fig. S5**). The shapes of the PL spectra are very similar to each other, but the intensity of Pt/P25-400 is much lower as compared with those of P25 and Pt/P25, which indicates that the recombination of photo-induced electron-hole pairs is greatly suppressed. This phenomenon may be caused by the formation of bond tail states.[13] The enhanced charge separation is believed to be the major reason for the improvement of photocatalytic activity.

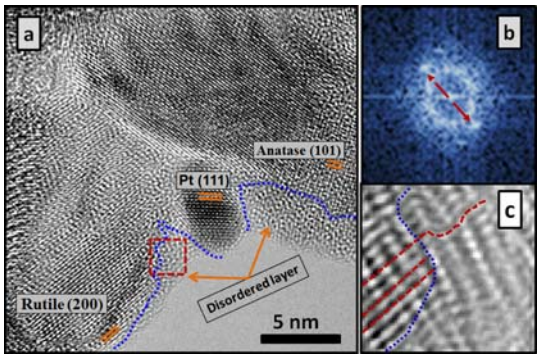

Figure 3. (a) HRTEM image of Pt/P25-400; (b) the FFT image of the area marked with red dash line box in (a); (c) Inverse Fast Fourier Transformation of image (b) performed on the red arrow pointed spots

The hydrogenated sample Pt/P25-400 was also characterized by HRTEM. From the image shown in **Fig. 3a** a disordered shell coating on both anatase and rutile crystalline cores could be observed, as marked by the blue dash line. Generally, the disordered shell is a typical morphology change of TiO_2 after hydrogenation[4,14]. To obtain more information of the disordered shell, we selected an area in **Fig. 3a** (red box) to perform the Fast Fourier Transform (FFT) and Inverse Fast Fourier Transformation (IFFT), the results of which are shown in **Fig. 3b**. The two bright spots in **Fig. 3b** (red arrow pointed) were selected to perform the IFFT; the resulted image is displayed in **Fig. 3c**. It is clearly found that the left part of the image in **Fig. 3c** divided by blue dash line presents an ordered and periodic arrangement of lattice; however, the right part shows greatly distorted lattice structure. By theoretical calculations and experiments, several groups thought that the enhancement of hydrogen production on hydrogenated TiO_2 is mainly contributed by the surface disordered layer. The distortion of crystal lattice results in the formation of the bond tailing of energy band, as seen directly in **Fig. 3c.**

In a summary, for the first time, we successfully synthesized the Pt-promoted TiO_2@TiO_{2-x} photocatalyst (Pt/TiO_2-x) *via* a facile H_2 spillover enhanced one-step hydrogenation with metallic Pt nanoparticles preloaded on TiO_2. Compared with the Pt/TiO_2 without treated by H_2 and the Pt/TiO_2(H_2) with the TiO_2 hydrogenated first, the catalysts Pt/TiO_2-x exhibit much better catalytic activity for water splitting. The optimal hydrogenation temperature is 400 ^{o}C. The as-proposed hydrogen spillover involved hydrogenation strategy is a feasible and highly efficient hydrogenation route. The generation of oxygen vacancy and the formation of band tail states during hydrogenation are responsible for its high catalytic activity due to the suppression of electron-hole recombination.

This work was supported by the National Natural Science Foundation of China (Nos. 21276184, U1332102) and the Specialized Research Fund for the Doctoral Program of Higher Education of China (No.20120032110014). The authors are also grateful to the Program of Introducing Talents of Discipline to University of China (No.B06006)

Notes and References

Collaborative Innovation Center for Chemical Science & Engineering (Tianjin), Tianjin Key Laboratory of Applied Catalysis Science & Engineering, School of Chemical Engineering & Technology, Tianjin University, Tianjin 300072 (P. R. China).
Tel/Fax: +86 22-2789-2275; E-mail: mengm@tju.edu.cn

Electronic Supplementary Information (ESI) available:[].See DOI: 10.1039/c000000x/

1. X. Chen, S. Shen, L. Guo and S. S. Mao, *Chem. Rev.*, 2010, **110**, 6503-6570.
2. R. Asahi, T. Morikawa, T. Ohwaki, K. Aoki and Y. Taga, *Science*, 2001, **293**, 269-271.
3. W. Choi, A. Termin and M. R. Hoffmann, *Angewandte Chemie International Edition in English*, 1994, **33**, 1091-1092.
4. X. Chen, L. Liu and P. Y. Yu, S. S. Mao, *Science*, 2011, **331**, 746-750.
5. (a) G. Wang, H. Wang, Y. Ling, Y. Tang, X. Yang, R. C. Fitzmorris, C. Wang, J. Z. Zhang and Y. Li, *Nano Lett.*, 2011, **11**, 3026-3033; (b)S. Hoang, S. P. Berglund, N. T. Hahn, A. J. Bard and C. B. Mullins, *J. Am. Chem. Soc.*, 2012, **134**, 3659-3662; (c) A. Naldoni, M. Allieta, S. Santangelo, M. Marelli, F. Fabbri, S. Cappelli, C. L. Bianchi, R. Psaro and V. Dal Santo, *J. Am. Chem. Soc.*, 2012, **134**, 7600-7603; (d) Z. Zheng, B. Huang, J. Lu, Z. Wang, X. Qin, X. Zhang, Y. Dai and M. H. Whangbo, *Chem. Commun.* 2012, **48**, 5733-5735.
6. (a) Z. Wang, C. Yang, T. Lin, H. Yin, P. Chen, D. Wan, F. Xu, F. Huang, J. Lin, X. Xie and M. Jiang, *Adv. Funct. Mater.*, 2013, **20**, 5444-5450; (b) Z. Wang, C. Yang, T. Lin, H. Yin, P. Chen, D. Wan, F. Xu, F. Huang, J. Lin, X. Xie and M. Jiang, *Energy Environ. Sci.*, 2013, **6**, 3007-3014.
7. R. Prins, *Chem. Rev.*, 2012, **112**, 2714-2738.
8. H. Zhu, Z. Qin, W. Shan, W. Shen and J. Wang, *J. Catal.*, 2004, **225**, 267-277.
9. Y. Li, D.-S. Hwang, N. H. Lee and S.-J. Kim, *Chem. Phys. Lett.*, 2005, **404**, 25-29.
10. (a) Z. Zhang, J. Long, X. Xie, H. Zhuang, Y. Zhou, H. Lin, R. Yuan, W. Dai, Z. Ding and X. Wang, *Appl. Catal. A: Gen.*, 2012, **425**, 117-124; (b) X. S. Li, W. Z. Li, Y. X. Chen and H. L. Wang, *Catal. Lett.*, 1995, **32**, 31-42.
11. D. A. Panayotov and J. T. Yates Jr, *Chem. Phys. Lett.*, 2007, **436**, 204-208.
12. M. Sathish, B. Viswanathan, R. P. Viswanath and C. S. Gopinath, *Chem. Mater.*, 2005, **17**, 6349-6353.
13. L. Liu, P. Y. Yu, X. Chen, S. S. Mao, and D. Z. Shen, *Phys. Rev. Lett.* 2013, **111**, 065505-065509
14. (a) *X. Chen,* L. Liu, Z. Liu, M. A Marcus, W. Wang, N. Oyler, M. Grass, B. Mao, P. Glans, P. Y. Yu, J. Guo and S. S. Mao. *Sci. Rep.* 2013, 3, 1510-1516; (b) T. Xia, X. Chen. *J. Mater. Chem. A,* 2013, **1**, 2983-2989